ARTICLE NO. 79-0209R

J80-099

Acoustic Suppression in a Pulsed Laser System

20001
30003
30012

B. N. Srivastava,* C. J. Knight,* and O. Zappa†
Avco Everett Research Laboratory, Inc., Everett, Mass.

The paper describes experimental and theoretical studies aimed at achieving acoustic suppression in a high-energy pulsed electric discharge laser system. Small-scale experiments were conducted for an open-cycle system having a sonic orifice plate upstream of the cavity and an acoustic horn and sidewall muffler downstream. The theoretical studies address the performance of the attenuators used for the experiments in both the linear and nonlinear acoustic response regimes. The linear regime is investigated by developing analytical solutions; whereas for the nonlinear regime, a "floating shock-fitting" technique is applied. Comparisons of the theoretical predictions with the experimental results are presented.

Introduction

FLOWING gas laser systems were a necessary step toward generating high average output power from a single cavity with good beam quality. In this paper we will be discussing a pulsed CO_2 gas laser configuration in which laser initiation energy is added in a short duration *e*-beam sustained electric discharge. In practice, there could be a large number of pulses spaced a fraction of a second apart in a pulse train. During the intrapulse time, waste-heated gas must be removed from the cavity and acoustic disturbances, caused by waste-heat deposition during the initiation process, must be damped to a low level in order to assure the medium will produce a high quality output beam at the succeeding pulse. For a CO_2 laser system operating at room conditions and with a 1 m path length between mirrors, a typical density homogeneity requirement is $(\delta\rho/\rho)_{rms} \leq 1 \times 10^{-3}$. This paper summarizes an experimental and theoretical study of an attenuator configuration meant to achieve the desired performance.

There are two basic categories of pulsed laser systems, depending on the system optimization criterion. Maximizing the average output power per unit mass in a pulse train is appropriate for open-cycle or blowdown facilities in which lasing mixture is stored at high pressure in tanks and one wants to get as much power from that fixed gas supply as possible. It typically involves low base flow Mach numbers (e.g., $M_s \sim 0.1$). More recently, interest has focused on closed-cycle systems in which maximizing average output power in a pulse train is the appropriate goal. This paper is concerned only with open-cycle systems.

The generic elements in an open-cycle configuration are shown in Fig. 1. Taking advantage of the high pressure at which the gas will typically be stored, a sonic orifice plate with highly underexpanded jets is used to define the upstream boundary of the flow channel. The mass flow through the channel is controlled by fixing the plenum pressure and temperature just upstream of the orifice plate. The pressure drop across the orifice plate is chosen to insure that no objectionable acoustic disturbances are transmitted into the plenum. Downstream of the laser cavity, there will be an acoustic attenutor section and ultimately the flow channel terminates with an opening to the surrounding environment.

An initial step in the process of establishing an acoustic suppression system is the generation of the temporal and spatial variations of the waves generated by the discharge in the laser cavity with no means of pressure wave attenuation. Considerable insight into the problem of acoustic wave suppression can be obtained by observing what happens after a single pulse in the laser cavity. The configuration considered is a 155-cm-long constant area flow channel with hard walls. The discharge region is 6 cm long and begins 1 cm downstream of the sonic orifice plate. This is followed by a 148-cm-long straight duct terminated by an opening to infinite surroundings. The sonic orifice plate reflects pressure waves whose strength and nature are determined by downstream conditions. The mass flow from the sonic orifice corresponds to an initial cavity Mach number of 0.2, and the laser initiation process, treated as instantaneous at $t=0$, generates initial shock waves with a pressure ratio of 1.5.

Typical early time wave histories for these conditions are depicted in Fig. 2. The laser initiation process generates shock waves, contact surfaces, and expansion waves which are sent upstream and downstream of the laser cavity. Expansion waves cross in the center of the lasing cavity and reflections of

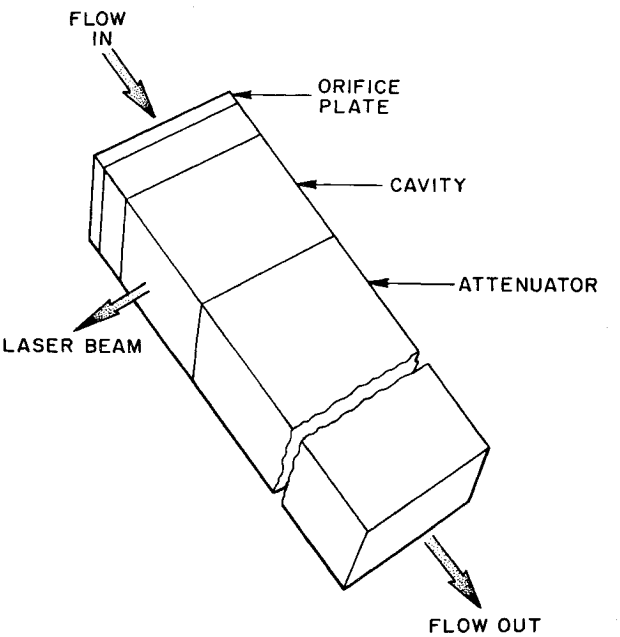

Fig. 1 Generic components of an open-cycle laser system.

Presented as Paper 79-0209 at the AIAA 17th Aerospace Sciences Meeting, New Orleans, La., Jan. 15-17, 1979; submitted Jan. 22, 1979; revision received Oct. 9, 1979.

Index categories: Lasers; Aeroacoustics; Analytical and Numerical Methods.

*Principal Research Scientist. Member AIAA.
†Principal Research Scientist.

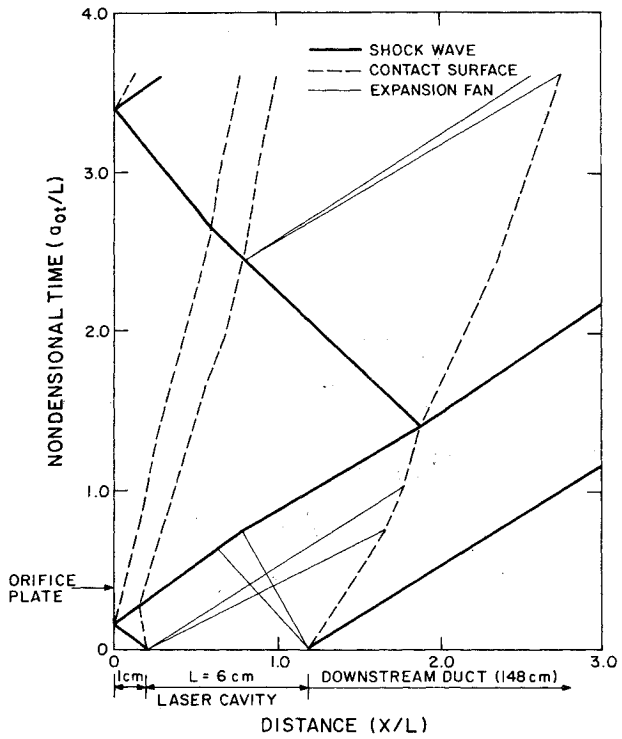

Fig. 2 Initial waves in the laser cavity (no attenuators).

the waves occur both off the upstream sonic orifice plate and off the contact surfaces. The sonic orifice plate, on interaction with an incoming shock wave, gives rise to a downstream propagating shock wave followed by a contact surface. Of particular significance is the strength of the upstream reflected shock wave and its interaction with the downstream contact surface. This interaction causes a reflected shock wave which bounces back and forth in the laser cavity between the contact surfaces. At times later than those shown in Fig. 2, there will also be a reflected wave from the open exit at the end of the flow channel. If one is not limited by a desired pulse repetition frequency, these waves will utimately decay by successive reflections and interactions among themselves. In practice, however, desired medium homogeneity must be achieved within the laser cavity in very short time in order to obtain high average output power (e.g., 10-20 acoustic transit times).

The preceding discussion emphasizes the need for a suitable downstream attenuator configuration in order to achieve acoustic suppression in a repetitively pulsed laser cavity. The technical content of this paper, however, will only be concerned with the single pulse situation, which is a first step toward achieving the goal of acoustic suppression for multipulse situations. The experimental and theoretical efforts for achieving this goal are described in the sections that follow.

The experimental effort consisted of utilizing a choked orifice plate as a wave reflector and an acoustic horn and finite capacity muffler as wave attenuators. The details of this flow device are given in Sec. II. Experimental results show that the initial cavity disturbances are successfully damped to a desired level. The theoretical efforts were directed toward developing and understanding the wave attenuation process in this flow device by using quasi-one-dimensional models of the primary elements. These models are validated by comparison with existing experimental and theoretical results from the literature. The details of this analysis are given in Sec. III. Finally, the results of a numerical simulation for the complete flow device are given in Sec. IV. Comparison of the pressure transducer measurements with theoretical predictions indicate that the quasi-one-dimensional modeling developed in this paper is adequate for predicting the response of the device.

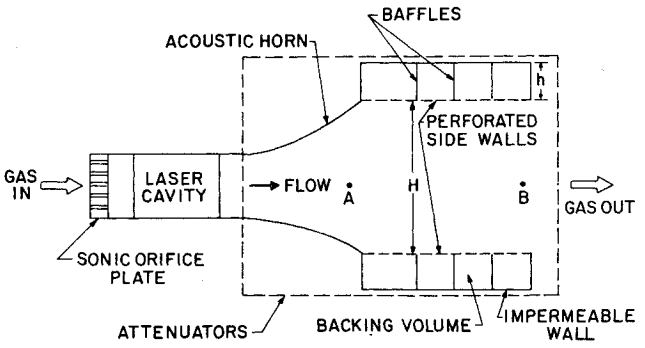

Fig. 3 Elements in an open-cycle pulsed laser system.

II. Experiments on an Acoustic Suppression System

Experimental development and verification of an acoustic suppression system was conducted on a subscale pulsed electric discharge laser. The device was operated in a blowdown mode with an underexpanded sonic flow plate upstream of the cavity as shown in Fig. 3. The pressure ratio across the flow plate was chosen to assure that all acoustic waves produced by the discharge would be reflected downstream. To assure rapid flow clearing between pulses, the cavity starts almost immediately downstream of the flow plate. Acoustic attenuators are placed downstream of the laser cavity with this arrangement.

In an open-cycle flow system, the gas is ultimately exhausted to the atmosphere and the impedance mismatch at this open exit is an important consideration in designing the acoustics system. A means of impedance matching as well as attenuating the acoustic waves was investigated in the experiment. Impedance matching involved the use of an exponential horn as a transition section between the laser cavity and a sidewall muffler section. The cross-sectional area at the end of the two-dimensional horn was about twice that in the cavity, and the horn length is large compared to the cavity length in the flow direction. The exponential horn reduces the strength of the acoustic signal at the entrance to the muffler, but it also introduces a delay in the arrival time of waves from the cavity. More will be said in later sections about the use of an acoustic horn and its probable impact on flow clearing time between pulses.

Acoustic attenuation takes place in a sidewall muffler section downstream of the horn. The flow channel height in the muffler is constant and all gas exhausts to the surrounding environment at the open end of this channel. That is, the muffler backing volume depicted in Fig. 3 is closed and no gas is removed from it by suction. The backing volume was divided into separate Helmholtz resonators by baffles placed perpendicular to the flow direction. The backing depth and open area ratio were varied linearly over the first 30% of the muffler length to achieve a gradual variation of impedance. The muffler configuration was selected to give good attenuation characteristics for frequencies of 300-1000 Hz.

The side panels on each wall between the flow channel and the backing volume consisted of a sandwich of porous material between two perforated plates. The plate nearest the flow was 20% open and the other plate was 45% open. The porous material was selected experimentally on the basis of maximum attenuation of the leading shock from the laser cavity. Figure 4 shows the performance of the muffler and its variation with the experimentally determined wall panel resistance in cgs Rayls at the panel midsection position.

A typical pressure history from the experimental setup is shown in Fig. 5. The upper trace is for a pressure transducer located 33 cm downstream of the flow plate at the entrance to the muffler. The first sharp peak is due to the leading shock which is generated by the electrical discharge in the cavity (340

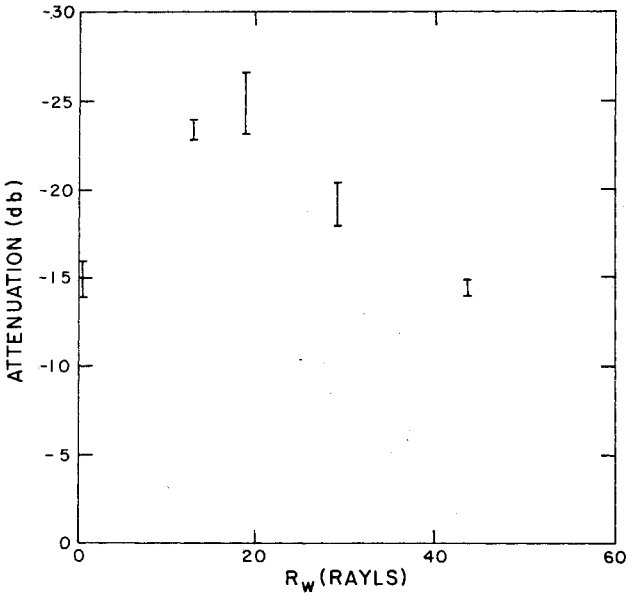

Fig. 4 Attenuator performance variation with effective wall resistance.

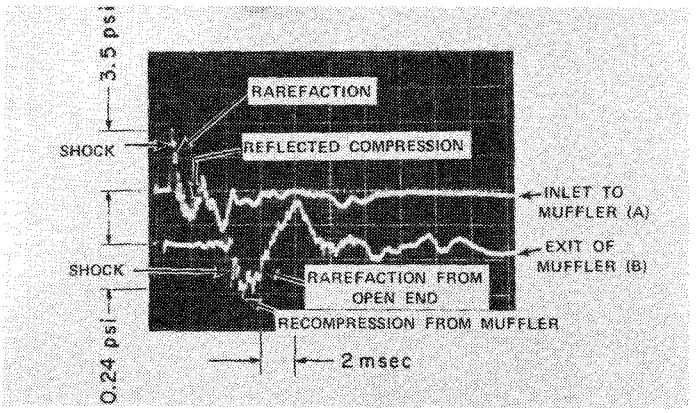

Fig. 5 Typical pressure transducer traces.

J/ℓ loading in a 3 N_2/1 CO_2/0.08 H_2 laser gas mixture at 300 K). The second pressure rise appears to be due to reflected expansion waves from the downstream hot/cold gas interface produced by the discharge. This was deduced from approximate x-t diagrams constructed from pressure histories from transducers at various locations in the laser system. The lower trace in Fig. 5 shows the pressure history at the exit of the muffler. This shows a relatively weak shock followed immediately by distributed compression waves.

Figure 6 shows a sequence of interferometer pictures depicting the wave history and flow clearing after a single pulse. Each picture represents a separate blowdown test, and the results were determined to be reproducible. Waves propagating transverse to the flow direction are clearly seen at early times. These arise because the anode and cathode rods are each displaced from the channel wall by about one-sixth of the channel height in the cavity. That is, the discharge is confined to the central two-thirds of the flow channel in the cavity region. This has been discussed previously in Ref. 2. The three vanelike objects in the upper portion of each picture are a portion of the e-beam shield used to confine the discharge. The upstream hot/cold gas interface is quite distinctive and clears at the flow speed. There is also an entropy wave seen at 9 ms after the discharge produced by a pressure wave interacting with the flow plate. It is located between the flow plate and the hot/cold gas interface.

The flow is relatively clear of disturbances, except for a separated layer evident in the flow-only condition as well, about 15 ms after the discharge. The separated layer was caused by a step in the wall contour that was later removed. Analysis of these interferograms shows that the desired homogeneity can be restored in a time consistent with pulse repetition frequencies of interest.

III. Theoretical Analysis

Quasi-One-Dimensional Flow Modeling

Quasi-one-dimensional flow modeling will be used in developing a theoretical basis for understanding the acoustic attenuation studies discussed in the preceding section. In this section, suitable one-dimensional models of the primary flow elements are developed and validated by comparison with

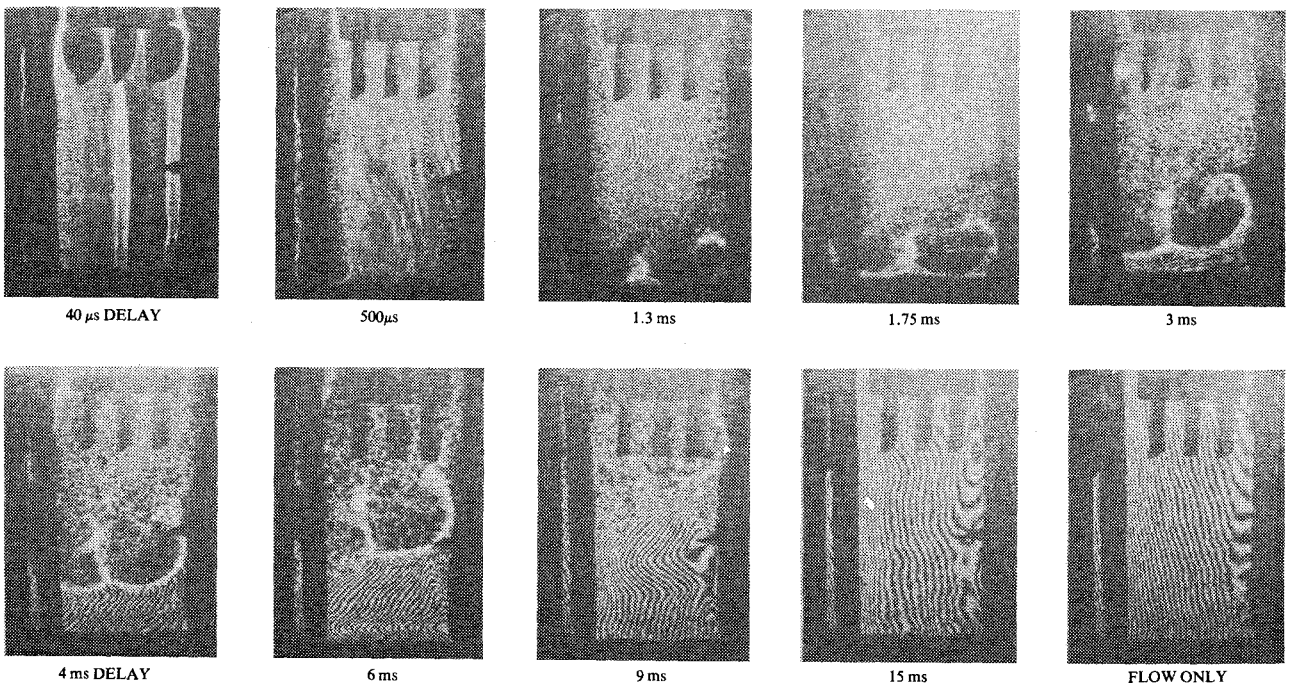

Fig. 6 Acoustic clearing in laser cavity.

theoretical and experimental results from the literature. Here the elements will be considered individually, rather than as part of a system. Theoretical predictions for the attenuator system will be given and compared with the experiment in the next section.

Equations expressing conservation of mass, momentum, and energy for unsteady, quasi-one-dimensional motion of gas in the flow channel are:

$$\frac{\partial}{\partial t}(\rho A)+\frac{\partial}{\partial x}(\rho u A)=m_1 \tag{1a}$$

$$\frac{\partial}{\partial t}(\rho u A)+\frac{\partial}{\partial x}(\rho u^2 A)+A\frac{\partial p}{\partial x}=m_2 \tag{1b}$$

$$\frac{\partial}{\partial t}(\rho A e)+\frac{\partial}{\partial x}(\rho u A e)+p\frac{\partial}{\partial x}(uA)=m_3 \tag{1c}$$

where A is the cross-sectional area of the duct and m_1, m_2, m_3 are source-sink terms. The form of these terms depends on the attenuator concept being modeled and will be discussed later. The gas is treated as ideal, therefore,

$$p=\rho RT, \quad e=RT/(\gamma-1) \tag{2}$$

where R is the gas constant and γ is the ratio of specific heats. Both are taken to be constant.

There will also be additional transient flow equations in the case of a sidewall muffler describing what takes place in the backing volume. These will be given later. However, Eqs. (1) adequately define the nature of the numerical problem to be addressed. Strong shock waves and contact interfaces will be produced by the discharge loading in the laser cavity and these will interact with each other during the attenuation process. With initial shock pressure ratios of about 1.5, the transient flow process is highly nonlinear at early times.

Numerical Solution

The time-dependent solutions to the flow equations are generated by a "floating shock-fitting" numerical technique[3] which utilizes a fixed piecewise uniformly spaced Eulerian grid system. The spacing in different regions is allowed to be different to improve computational efficiency. Flow discontinuities such as shock waves, contact interfaces, and gradient discontinuities are allowed to "float" through the Eulerian grid and are updated using a local characteristics procedure.[4] Away from flow discontinuities, a second-order-accurate MacCormack predictor-corrector scheme is used to advance flow information in time at Eulerian grid points. The advantage of using a MacCormack scheme is its accuracy and the ease with which it can be implemented. Numerical stability of this explicit finite differencing scheme limits the time step size according to the Courant-Friedricks-Lewy criterion.[3]

In the problem considered here, one is interested not only in strong waves involved at early times but also very weak waves, since the medium homogeneity must be restored to $(\delta\rho/\rho)_{\text{rms}} \sim 10^{-3}$ at the end of the intrapulse time. The accuracy of the numerical scheme over a wide range of wave strengths is therefore an important issue. One difficulty encountered during early numerical experiments was numerical errors generated at grid points where the source-sink terms in Eqs. (1) were discontinuous. Flow derivatives are discontinuous at such juncture points and this led to error in using the MacCormack scheme. To alleviate this difficulty, a local characteristics update scheme was implemented at the juncture points. With this modification the algorithm was found to be adequately accurate.

Boundary Conditions

The boundary conditions of interest here involve a choked flow plate upstream of the laser cavity and an open exit to an infinite environment at the downstream end of the flow channel. These are typical for an open-cycle laser system operating at near-ambient pressure in the cavity.

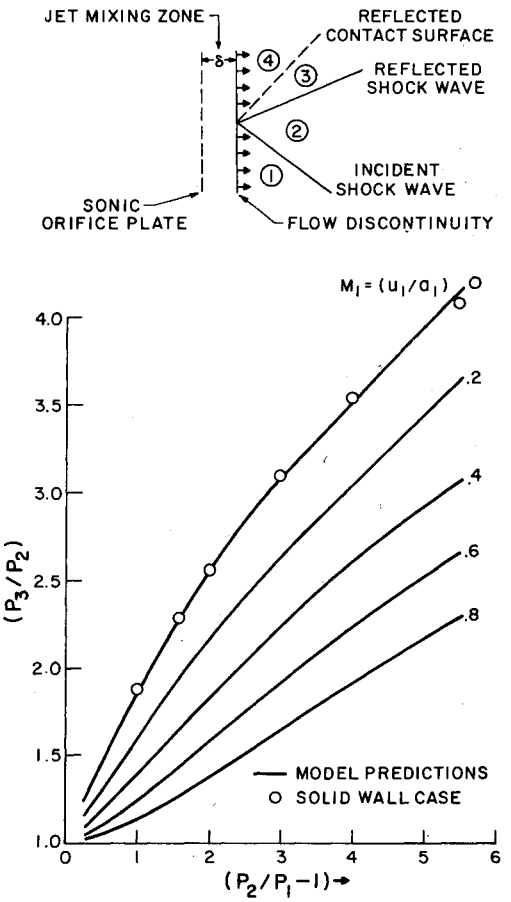

Fig. 7 Sonic orifice plate modeling.

In the past (e.g., Ref. 5), there has been a practice of modeling choked flow plates as if they behave like a rigid wall when interacting with pressure waves in the duct, with a provision to include the necessary mass injection at a point downstream of the flow plate. The present paper uses a more realistic treatment which assumes that the flow plate holds the mass flux and stagnation temperature fixed at the inlet to the laser cavity but that the pressure at the flow plate is fixed by downstream conditions. A local method of characteristics, which utilizes the compatibility relation along the Mach line moving upstream to the flow plate, is used to determine conditions at the flow plate. The "rigid wall" treatment will give approximately the same result as this characteristics treatment at low-cavity Mach number, but not more generally.

The treatment just outlined is essentially tantamount to assuming that there is a stationary flow discontinuity in place of the choked orifice plate. This will be a valid idealization only if the distance δ in Fig. 7, within which the jets issuing from individual orifices coalesce into a uniform flow, is small compared to cavity dimensions. Small values of δ are typically a design goal in practice, because that distance directly affects the required intrapulse time and hence the achievable average output power of a repetitively pulsed laser system. This is achieved by drilling many uniformly and closely spaced small diameter holes in a plate.

The method of characteristics cannot be used to treat the interaction of another flow discontinuity with the flow plate. Using the same idea of constancy of mass flow and stagnation temperature, it can be demonstrated that the only possible wave configuration when a shock interacts with a flow plate is a reflected shock followed by a contact discontinuity as shown in Fig. 7. Setting up the necessary jump conditions across the

shocks, the contact interface, and the stationary "flow plate discontinuity" leads to the predicted reflected shock strengths shown in Fig. 7 as a function of the incident shock strength. The Mach number just before shock arrival M_I defines different mass injection rates. These results are for $\gamma = 1.4$. Note that the strength of the reflected shock would be significantly lower than that predicted by a model which treats the flow plate as a rigid wall for $M_I > 0.05$.

Turning to the open exit, the flow code was set up to treat the general quasi-one-dimensional boundary conditions associated with a subsonic, sonic, or supersonic exit flow. The treatment for each of these cases, using a local method of characteristics, is discussed by Rudinger.[6] Interaction of flow discontinuities with the open exit are also allowed in the code.[6] In the cases actually run, there was only subsonic outflow at the end of the flow channel, and the appropriate steady-state boundary conditions in that case is that the static pressure be equal to the external ambient pressure. Time delay effects in establishing the steady-state boundary condition at the open exit[6] were not accounted for in the code because they were expected to be negligible.

Acoustic Horn

A properly designed acoustic horn is known to be a successful radiator of a sinusoidal wave train if the horn length is long compared to the wavelength. However, its response to pressure pulses is not as well known. Analytical and computational techniques have been used to study the interaction of pressure pulses with an exponential horn in both the linear and nonlinear response regimes. The results of this study can only be summarized briefly here due to lack of space.

Consider first the linear response of an exponential horn to a step input or shock wave. The analysis consisted of solving the linearized transient flow equations using Laplace transform techniques for a horn typified by the area ratio $e^{2\delta}$ where $\delta = mL/2$, m is the flare constant, and L is the length of the horn. The resulting response to a step input is shown schematically in Fig. 8. The incident shock of strength Δp_i gives rise to a transmitted wave consisting of a shock, with amplitude reduced by the square root of the area ratio (i.e., $e^{-\delta}\Delta p_i$), followed by a distributed expansion wave. The reflected wave is a distributed rarefaction. Note that the strength of the composite transmitted wave and the reflected wave are the same as if the incident shock had interacted with an area discontinuity of the same area ratio as the horn. The exponential horn merely distributes the waves over a distance comparable to 2-3 horn lengths.

The analysis was repeated for a finite duration pulse of rectangular and triangular waveforms. If the incident pulse has a temporal duration long compared to the acoustic transit time through the horn, this analysis shows that the composite (ensemble of all waves) reflected and transmitted waves have the same strengths as if the incident wave had interacted with an area discontinuity of the same area ratio. On the other hand, when the incident wave has temporal duration short compared to the acoustic transit time through the horn, the reflected wave strength becomes small and the transmitted waveform becomes similar to the incident waveform, but has amplitude reduced by the square root of the area ratio. These conclusions should be valid for any input pressure waveform that has a well-defined finite duration.

In the case of the exponential horn used in the experiment discussed in Sec. II, the horn length is about five times the cavity length. A representative input waveform from the laser cavity is a triangular pulse consisting of a shock wave followed by a linear decay in pressure back to the level before the shock. Response in both the linear and nonlinear regimes were calculated for this case. The reflected wave strengths obtained using linear and nonlinear theories are shown in Fig. 9. The change in the Riemann invariant Q has been normalized by the change in the Riemann invariant P across the incident shock wave, and the gas is taken to be stationary and

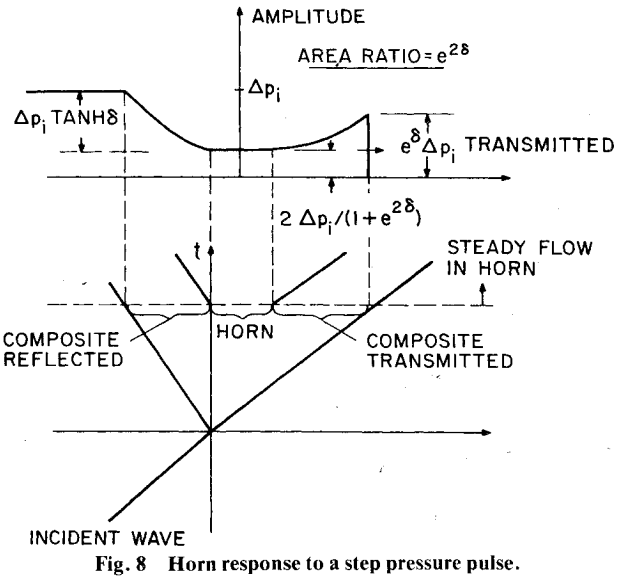

Fig. 8 Horn response to a step pressure pulse.

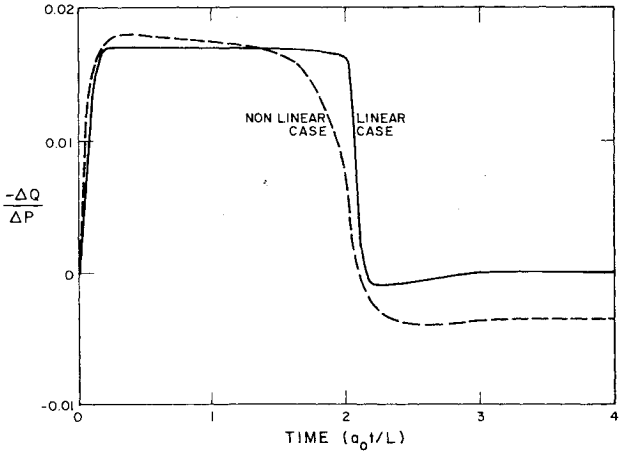

Fig. 9 Horn response (reflection) to a triangular pulse of duration $\tau = 0.2$.

to have sound speed a_0 before the pressure pulse arrives. The linear and nonlinear results are in reasonable agreement at conditions which approximate those for the experiment discussed in Sec. II.

The reflected wave is seen to be sharply terminated by a compression of duration comparable to the incident pressure pulse. This is an undesirable feature for laser applications because it implies significant optical aberration in the cavity at a time well after the laser pulse. Ideally, the wavelength of acoustic waves arriving in the cavity at late times should be very long compared to the cavity. Presumably this compressive component can be minimized or eliminated in the laser system by carefully impedance matching with the sidewall muffler downstream.

Sidewall Muffler

We have considered both infinite and finite capacity backing volume in theoretically modeling sidewall mufflers. Infinite backing volume is considered as a first step toward validating the quasi-one-dimensional modeling by comparison with independent shock tube experiments.[7,8] Simple scaling relations for a sidewall muffler also result from that theory. The effects of finite backing volume in the laser experiment were found to be quite significant and necessitated developing a new more general theory. The quasi-one-dimensional model of a finite capacity muffler is derived below.

It will be adequate for this discussion to assume that the channel height H, the backing depth h, and the open-area ratio of the perforated sidewalls α are all constants (cf., Fig. 3). The perforated walls are taken to be very thin. Also, it will be assumed that the velocity in the backing volume is zero—as can be achieved with baffles and/or porous packing material. Integration of two-dimensional equations over the flow channel and the backing volume then leads to the following system of transient quasi-one-dimensional flow equations:

$$\frac{\partial \rho}{\partial t} + \frac{\partial (\rho u)}{\partial x} + \frac{2\alpha}{H}\dot{m} = 0 \tag{3a}$$

$$\rho\left(\frac{\partial u}{\partial t} + u\frac{\partial u}{\partial x}\right) + \frac{\partial p}{\partial x} + \frac{2\alpha}{H}\dot{m}(u_w - u) = 0 \tag{3b}$$

$$\rho c_v\left(\frac{\partial T}{\partial t} + u\frac{\partial T}{\partial x}\right) + p\frac{\partial u}{\partial x} + \frac{2\alpha}{H}\dot{m}\left[c_p T_w + \frac{(u_w - u)^2 + v_w^2}{2} - c_v T\right] = 0 \tag{3c}$$

$$\frac{\partial \rho_b}{\partial t} - \frac{\alpha}{h}\dot{m} = 0 \tag{3d}$$

$$\frac{\partial}{\partial t}(\rho_b c_v T_b) - \frac{\alpha}{h}\dot{m}\left(c_p T_w + \frac{u_w^2 + v_w^2}{2}\right) = 0 \tag{3e}$$

where unsubscripted variables apply in the flow channel, subscript w denotes values in the perforated wall orifices, and subscript b denotes values in the backing volume. Equations (3a-c) represent the conservation of mass, momentum, and energy in the flow channel, respectively, and are of the form given by Eqs. (1), while the last two represent mass and energy conservation within the backing volume. Further discussion of quasi-one-dimensional modeling with mass, momentum, and energy exchange at the bounding walls is given by Shapiro.[9]

First consider outflow from the channel to the backing volume. If the process is taken to be locally quasi-steady, it is intuitively plausible that the stagnation temperature and entropy will be preserved in the channel flow and that the channel acts as a plenum for the flow through the orifices in the sidewalls. Quasi-steady modeling will be valid if the orifice diameter and the distance between perforations is small compared to, say, the channel height or cavity length in the flow direction. This leads to

$$\dot{m} = C_{D_+}\frac{\gamma p}{\gamma - 1}\sqrt{\frac{2}{c_p T}\left(\frac{p_b}{p}\right)^{2/\gamma}\left[1 - \left(\frac{p_b}{p}\right)^{\gamma - 1/\gamma}\right]}$$

$$u_w = u$$

$$c_p T_w + \frac{u_w^2 + v_w^2}{2} = c_p T + \frac{1}{2}u^2 \tag{4}$$

where C_{D_+} is the discharge coefficient for outflow. In the case of inflow from the backing volume to the channel, it is plausible to require an isentropic decompression of the backing volume in the context of locally quasi-steady modeling. Thus,

$$\dot{m} = C_{D_-}\frac{\gamma p_b}{\gamma - 1}\sqrt{\frac{2}{c_p T_b}\left(\frac{p}{p_b}\right)^{2/\gamma}\left[1 - \left(\frac{p}{p_b}\right)^{\gamma - 1/\gamma}\right]} \tag{5}$$

$$u_w = 0$$

$$c_p T_w + \frac{u_w^2 + v_w^2}{2} = c_p T_b$$

where C_{D_-} is the discharge coefficient for inflow. In practice, the discharge coefficients will be affected by grazing flow over the orifices.[10]

When the backing volume is very large (i.e, $h/H \to \infty$), Eqs. (3c) and (3d) imply that ρ_b and p_b are constant and these equations can be deleted. The form of the remaining equations indicates that the shock decay process in the muffler section ($x > 0$) is expected to be correlatable in terms of the incident shock Mach number M_s, the nondimensional penetration distance $\alpha X_s/D$ where D is the hydraulic diameter, and the ratio of specific heats γ. Shock tube experiments with infinite capacity sidewall mufflers have been performed by Szumowski[7] and by Wu and Ostrowski.[8] Both use air or $\gamma = 1.4$. Their results are replotted in Figs. 10 and 11 as M_s vs $\alpha x_s/D$. Szumowski used a circular shock tube with perforations uniformly distributed around the periphery of the muffler section and gave results for a range of open-area ratios. Figure 10 shows that this data can be collapsed in terms of the correlation variables. Wu and Ostrowski used a square cross section tube with perforations on only two opposed walls and published results for only one open-area ratio. The reasonable comparison between Figs. 10 and 11 results if α is interpreted to be a peripheral average open-area ratio as expected on the basis of theory; i.e., half the open-area ratio on the two perforated sidewalls for a square shock tube. This resolves an apparent discrepancy between the two experimental studies (cf., discussion after Ref. 8).

Theoretical predictions using our one-dimensional model for $2h/H \to \infty$ are also shown on these figures. The discharge coefficient in Eqs. (4) and (5) were chosen to give the best fit of experimental results with $C_{D_+} = C_{D_-}$ and constant. The best fit resulted for a discharge coefficient of 0.6 in Fig. 10 and 0.9 in Fig. 11. Both are plausible values for square-edged orifices and situations in which grazing flow effects are not important,[10] as should be true in these experiments. Also, since the fit is good for a significant range of $\alpha x_s/D$ values, the theory cannot be said to fit only because there is an adjustable parameter in it.

An interesting conclusion can be drawn from Figs. 10 and 11. Roughly speaking, the muffler length in a laser system is chosen to assure that the reflected wave, produced by pressure pulse interaction with the open end, will not produce unacceptable medium inhomogeneity when it returns to the cavity. Based on these figures, the two-pass attenuation through a

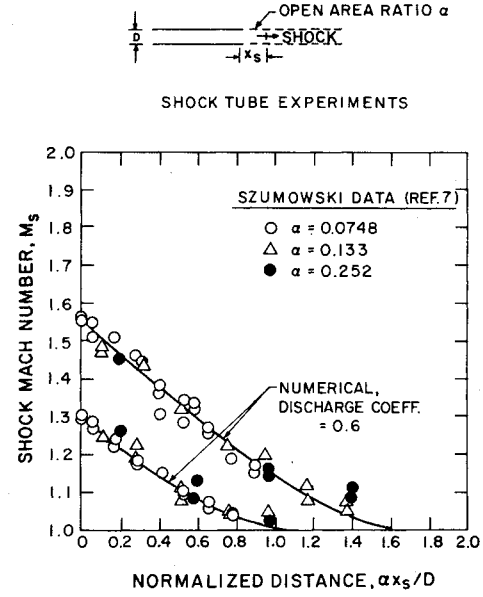

Fig. 10 Numerical predictions for infinite capacity muffler (circular section).

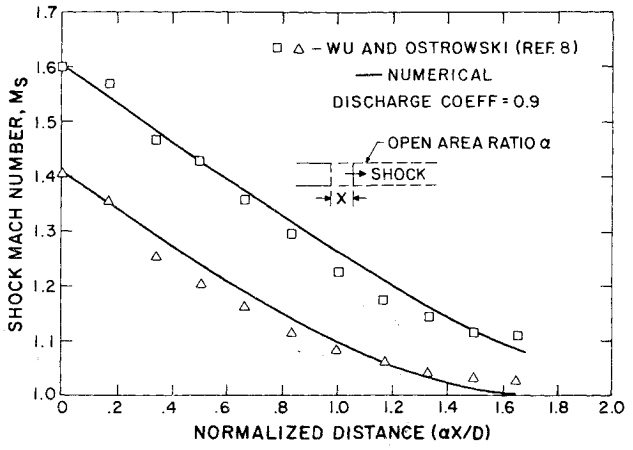

Fig. 11 Numerical prediction for an infinite capacity muffler (square section).

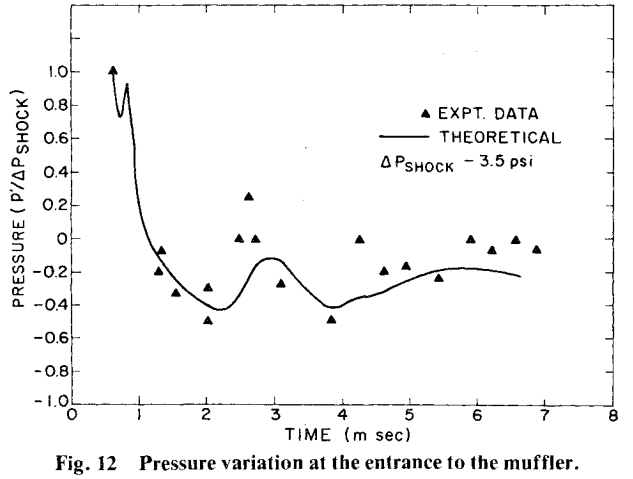

Fig. 12 Pressure variation at the entrance to the muffler.

muffler is determined by its L/D ratio for given initial shock Mach number and γ. Therefore, the required muffler length scales with the hydraulic diameter of the flow channel. For a two-dimensional channel, $D=2H$. It is also evident that $2h/H$ is the relevant parameter characterizing the effects of finite backing volume. The size of the muffler will be minimized by placing it in the duct section with a hydraulic diameter as small as possible. This is one argument for avoiding the use of an exponential horn in the experiment discussed in Sec. II.

IV. Comparison of Theory with Experiment

A comparison of the theoretical predictions with experimental data for the full acoustic suppression system is shown in Figs. 12 and 13. These results were obtained by using an effective open-area ratio for the muffler (i.e., product of open-area ratio α and discharge coefficient C_D), which was determined by a series of numerical calculations. The basic technique to determine the effective open-area ratio was to match the numerically predicted strength of the leading shock to that obtained experimentally at the exit of the muffler. This results in an effective open-area ratio of 6% at these conditions. The effective open area is significantly less than the geometric open area of the sidewall panel due to the resistance of the porous material packed into it as described in Sec. II. The effect of resistance over a restricted range of throughflow speeds is essentially the same as for a reduced, but constant, orifice discharge coefficient.

Figure 12 shows the pressure variation at transducer A, shown in Fig. 3, which is located at the exit to the acoustic horn. The pressure perturbation p' at the transducer is normalized by the initial shock overpressure (experimental Δp_{shock}) at that point. The theory agrees qualitatively with the

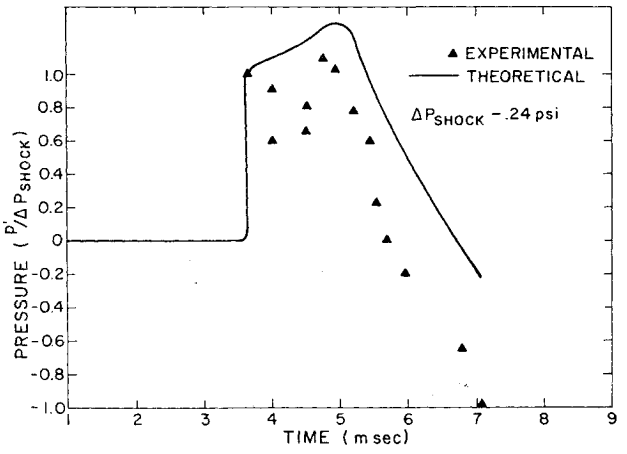

Fig. 13 Pressure variation at the exit to the muffler.

experimental results. However, there are quantitative discrepancies, especially the amplitude of the recompression wave at 2-3 ms in Fig. 12. The origin of that wave was discussed in Sec. II. Shock interaction with the muffler produces a reflected rarefaction wave. Interaction of that rarefaction wave with the downstream hot/cold gas interface, caused by the confined discharge loading and which is near the beginning of the horn, will, in turn, produce a compression wave reflected back to transducer A. It appears the theoretical modeling needs to be improved, but it is not clear how on the basis of available information. One likely possibility is that a more detailed model is required for the perforated sidewall panel used in the experimental setup, accounting for the different open area of the two plates in the panel sandwich and the resistance of the porous material between those plates.

Figure 13 shows the pressure variation at the exit to the muffler at transducer location B (Fig. 3). The pressure perturbation (p') is normalized by the shock overpressure at that point. It is observed from this figure that the time required for the shock to reach the end of the muffler is predicted well by the theory. The theoretical results show a compression wave arriving behind the shock and then a rarefaction apparently from the open end of the system. The qualitative comparison between theory and experiment seems to be reasonably good.

Ideally, we should compare theoretical predictions with experimental measurements in the laser cavity, since disturbances therein are really of primary interest. There are some basic problems in doing this. It is quite difficult to make pressure measurements in the cavity of a pulsed electric discharge laser because arcing to the transducer is highly probable and will destroy the transducer if it occurs. Interferometric measurements are also not ideal because there are significant two-dimensional phenomena taking place in the cavity, such as the transverse acoustic waves seen in Fig. 6 and discussed in Ref. 2. Any attempt at comparing theoretical predictions with interferograms was precluded by program schedule constraints.

A few comments on the use of acoustic horns can be made on the basis of the experimental and theoretical studies. The reflected wave from an exponential horn associated with a triangular input signal is shown in Fig. 9. The leading rarefaction and the trailing compression wave are both of duration comparable to the temporal duration of the input pressure pulse. That is, they produce a disturbance in the cavity of dimension comparable to the cavity length in the flow direction. This is precisely the sort of reflected wave one should avoid in laser applications because they generally lead to longer flow clearing times between pulses. This reflected wave was observed experimentally by a pressure transducer near the inlet to the horn. Another point is that the horn really does no attenuation. It is true that the strength of a shock is

reduced by the square root of the area ratio, but if the transmitted shock were reflected back through the horn (with no losses) it would return to its original strength when it reached the cavity.

An acoustic horn affects attenuator performance in two ways. First, it increases the distance from the cavity to the sidewall muffler, which would be expected to increase the intrapulse clearing time. It also increases the flow channel height in the muffler section by its area ratio. The sidewall muffler studies indicate that the muffler dimensions required to give a given level of attenuation scale in proportion to the flow channel height. Thus, use of the exponential horn in the experiment roughly doubled the muffler size required. Unless flow issues dictate otherwise, the use of acoustic horns in pulsed lasers is of questionable value.

V. Conclusions

This paper has investigated the pressure wave suppression in a pulsed electric discharge laser system. An experimental investigation of the pressure wave attenuation for one particular downstream attenuator configuration consisting of a sonic orifice plate, an acoustic horn, and a finite capacity muffler was carried out for a single pulse. Theoretical investigations of the performance of individual attenuators used in the expeimental setup were carried out for both linear and nonlinear regimes. A numerical simulation of the complete laser system based on quasi-one-dimensional modeling was also used to predict the attenuation of various pressures waves within the system. Comparison of the theoretical predictions with experimental observations are presented. Based on the present theoretical and experimental studies, the following conclusions have been reached:

1) For an open-cycle laser system, there is a large impedance mismatch between the laser cavity and the external environment into which the laser gas is dumped. This impedance mismatch implies strong reflection of acoustic waves back into the cavity from the open exit. A finite length and finite capacity muffler is an effective means of attenuating shock waves and of reducing the waves reflected back into the cavity due to the impedance mismatch at the open end.

2) An analytical/computational means to analyze acoustic waves in the flow direction in a complete laser system is developed and is shown to predict reasonably well the experimental observations.

3) The use of an acoustic horn in a pulsed laser attenuator system appears questionable. It increases the required size of the attenuator downstream, which scales with the flow channel height, and, as implemented here, introduces a time delay in waves from the cavity reaching that attenuator.

Acknowledgment

The theoretical work reported in this paper was supported by Avco Everett Research Laboratory, Inc., internal research and development funds and the experimental tests were supported by the Army under contract No. DAAK-40-75-C-1272.

References

[1] Born, M. and Wolf, E., *Principles of Optics*, Pergamon Press, New York, 1970.

[2] Knight, C. J., "Transverse Acoustic Waves in Pulsed Lasers," AIAA Paper, Cambridge, Mass., Nov. 1978.

[3] Roache, P. J., *Computational Fluid Dynamics*, Hermosa Publishers, Albuquerque, N. Mex., 1972.

[4] Moretti, G., "A Critical Analysis of Numerical Techniques: The Piston Driven Inviscid Flow," Polytechnic Institute of Brooklyn, PIBAL Rept. No. 69-25, 1969.

[5] Ausherman, D. R., Alber, I. E., and Baum, E., "Acoustic Suppression in a Pulsed Chemical Laser," AIAA Paper 78-237, Huntsville, Ala., Jan. 1978.

[6] Rudinger, G., *Nonsteady Duct Flow: Wave Diagram Analysis*, Dover Publications, New York, 1955.

[7] Szumowski, A. P., "Attenuation of a Shock Wave Along a Perforated Tube," Shock Tube Research, Proceedings of 8th International Shock Tube Symposium, edited by J. L. Stollery, A. G. Grayson, and P. R. Owen, Chapman and Hall, London, 1971.

[8] Wu, J.H.T. and Ostrowski, P. P., "Shock Attenuation in a Perforated Duct," Shock Tube Research, *Proceedings of 8th International Shock Tube Symposium*, edited by J. L. Strollery, A. G. Grayson, and P. R. Owen, Chapman and Hall, London, 1971.

[9] Shapiro, A. H., *Compressible Fluid Flow*, Ronald Press, New York, 1953, Chap. 8.

[10] Rogers, T. and Hersh, A. S., "Effect of Grazing Flow on the Steady-State Resistance of Squared-Edged Orifices," *Progress in Astronautics and Aeronautics*, Vol. 44, edited by I. R. Schwartz, AIAA, New York, 1976.